Available online at www.sciencedirect.com
ScienceDirect
Comparative Biochemistry and Physiology, Part D 3 (2008) 118–127
CBP
www.elsevier.com/locate/cbpd

Natural feeding influences protein expression in the dogfish shark rectal gland: A proteomic analysis

W. Wesley Dowd [a,*], Chris M. Wood [b,c], Makiko Kajimura [b,c], Patrick J. Walsh [b,d], Dietmar Kültz [a]

[a] *Physiological Genomics Group, Animal Science Department, University of California, Davis, 1 Shields Ave., Davis, CA 95616 USA*
[b] *Bamfield Marine Sciences Centre, Bamfield BC V0R 1B0 Canada*
[c] *Department of Biology, McMaster University, 1280 Main St. West, Hamilton, ON L8S 4K1 Canada*
[d] *Department of Biology, University of Ottawa, 30 Marie Curie, Ottawa, ON K1N 6N5 Canada*

Received 27 October 2007; received in revised form 27 November 2007; accepted 28 November 2007
Available online 8 December 2007

Abstract

The rectal gland is the principal salt-secreting organ in elasmobranchs, yet its functional response to normal physiological variation (e.g., due to feeding, stress) has only recently been examined. To complement studies on acid-base, digestive, and osmoregulatory physiology in response to natural feeding, we investigated protein-level responses in the rectal gland of spiny dogfish (*Squalus acanthias*) 6 h, 20 h, and 5 days (reference control) after a meal. Our objective was to identify proteins involved in regulation of osmoregulatory and metabolic processes in response to feeding. Proteins were separated by two-dimensional gel electrophoresis, and protein spots that were significantly up- or down-regulated >2 fold (i.e., abundance increased more than 100% or decreased more than 50%) were detected using gel image analysis software. Of 684 proteins analyzed on 2D gels, 16 proteins changed significantly 6 h after feeding vs. 5 day controls (5 decreased; 11 increased), and 12 proteins changed >2 fold 20 h after feeding vs. 5 day controls (2 decreased; 10 increased). Thirteen of these proteins were identified using mass spectrometry and classified into functional pathways using the PANTHER bioinformatics database. Rectal gland proteins that were regulated following feeding fell into three main categories: cytoskeletal/muscular (e.g., tropomyosin alpha chain, transgelin), energy metabolism (e.g., malate dehydrogenase, ATP synthase), and nucleotide metabolism (nucleoside diphosphate kinase). The data also revealed that previously documented increases in the activity of isocitrate dehydrogenase after feeding are at least partially due to increased abundance of a cytosolic, NADP-dependent isoform of this enzyme. One of the primary components of the rectal gland's response to feeding appears to be maintenance of the cellular supply of energy, which would be necessary to fuel increased activities of enzymes involved in salt secretion and oxidative metabolism in the rectal gland following a meal.

Keywords: Dogfish shark; *Squalus acanthias*; Rectal gland; Feeding; Isocitrate dehydrogenase; Voltage-dependent anion channel; MALDI-TOF mass spectrometry; Proteomics

1. Introduction

The mechanism of salt secretion by the elasmobranch rectal gland has been the subject of study for decades (for reviews, see Shuttleworth, 1988; Silva et al., 1990; Riordan et al., 1994; Silva et al., 1996; Olson, 1999; Hazon et al., 2003). In many cases the gland has been studied in isolation, for example with *in vitro* preparations, leading to a sound understanding of the mechanisms of salt secretion at the cellular and organ levels. In recent years, several studies have begun to (re)address the gland in the context of how it integrates into the overall osmoregulatory strategy of the organism (particularly in the dogfish shark, *Squalus acanthias*), especially in dealing with the salt load associated with feeding. While volume loading in itself is a powerful activating stimulus (Solomon et al., 1984a,b; Solomon et al., 1985), it now appears that a variety of other post-prandial signals may be involved, acting either directly or through neurohumoral pathways. These include plasma NaCl or ionic strength (MacKenzie et al., 2002) acting via a polyvalent cation receptor (Fellner and Parker, 2002, 2004), and the systemic alkaline tide resulting from stomach acid secretion (Wood et al., 2005; Shuttleworth et al., 2006; Wood et al., 2007a,b). Furthermore, feeding also leads to a substantial activation of rectal gland metabolic pathways that support the considerable ATP demand

* Corresponding author. Tel.: +1 530 752 8659; fax: +1 530 752 4154.
E-mail address: wwdowd@ucdavis.edu (W.W. Dowd).

1744-117X/$ - see front matter © 2007 Elsevier Inc. All rights reserved.
doi:10.1016/j.cbd.2007.11.003

posed by the Na^+/K^+-ATPase as it energizes active NaCl secretion. In particular, increases in activities of Na^+/K^+-ATPase, β-hydroxybutyrate dehydrogenase (β-HBDH), NADP-dependent isocitrate dehydrogenase (IDH), citrate synthase (CS), lactate dehydrogenase (LDH), alanine aminotransferase (AAT), aspartate aminotransferase (DAT) and glutamine synthetase (GS) were noted over 6 to 48 h postfeeding (Walsh et al., 2006). However, the patterns of enzyme activity were diverse with respect to the individual enzymes and time courses. For example, Na^+/K^+-ATPase showed two activity peaks at 6 and 48 h, whereas some enzymes showed only an early activation (e.g., β-HBDH at 6 h), some showed an early activation at 6 h that continued to rise to a peak at 20 h (e.g., LDH and IDH), while still others showed only a late activation (e.g., CS at 30 h). These results suggest a complex metabolic regulatory network that possibly involves both rapid post-translational activation of pre-existing enzymes, and transcriptional/translational activation that actually elevates protein/enzyme titers.

The dogfish shark has also recently proven to be an excellent model for comparative tissue proteomics in a "non-model" organism because, generally, inter-tissue variation in the shark proteome appears to be more limited than in mammals (Lee et al., 2006). Notably, this study compared osmoregulatory tissues with non-osmoregulatory tissues in an effort to understand what proteins are expressed in common by tissues that subserve an osmoregulatory function. In particular, it was discovered that osmoregulatory tissues (kidney, intestine, gill and rectal gland) shared enrichment in proteins of the pathways for energy and urea metabolism and the Rho-GTPase/cytoskeleton pathway, relative to non-osmoregulatory tissues (heart and brain) (Lee et al., 2006). More generally, proteomic techniques, in a manner analogous to transcriptomic approaches (e.g., cDNA microarrays), allow characterization of far more proteins simultaneously than traditional Western blot or protein activity approaches, offering the possibility to assess the regulation of numerous proteins, including those not anticipated to change. In combination with Western blots/etc, this discovery-driven proteomics approach is useful for unearthing new biological mechanisms and pathways involved in physiological adaptation, as well as possible interactions among biological pathways.

With this background in mind, the current study aimed to apply a similar proteomics approach to that of Lee et al. (2006) to examine the effects of feeding on dogfish shark rectal gland protein expression. Given the specific previous information obtained for this model, we were able to both: 1) test specific hypotheses regarding metabolic regulation in the dogfish rectal gland (e.g., that the increase in IDH activity is accomplished at least in part via increases in enzyme quantity); and 2) take a discovery-based approach to better understand the activation of an interesting and complex tissue by the simple but biologically important act of feeding.

2. Materials and methods

2.1. Experimental animals

Rectal gland tissue was harvested from the same set of experimental animals as described in the digestive physiology study of Wood et al. (2007a). In brief, dogfish sharks (*S. acanthias*) were collected from Barkley Sound, British Columbia and were held as a large group (~120 animals) in a 200,000 L circular indoor tank served with running seawater at the experimental temperature (11±1 °C), salinity (32±1 ppt), and pH (7.90±0.15). After several weeks, the dogfish were feeding readily, and a regime was implemented in which food was provided at 96 h intervals (freshly thawed, de-headed whole hake, *Merluccius productus*). A feeding frenzy invariably ensued, and all of the food was consumed within 30 min. The ration supplied at each feeding was 3% of the estimated mass of all the dogfish in the group tank. With practice, it was possible to discern which dogfish had fed based on the bulging profile of the abdomen, and at 1 h after feeding, these animals were caught and placed in individual 40 L polyurethane-coated wooden boxes served with a seawater flow of 1 L min^{-1}. Based on gut content measurements at autopsy, the average mass of food consumed on the single meal was 5–6% of body mass. In this manner, a group of animals (1.5–2.8 kg; 14 males, 1 female) were set aside for sampling at 6 h (N=5), 20 h (N=5), and 120 h (5 days, N=5) post-feeding. As digestion was essentially completed and the gastro-intestinal tract almost empty at 5 days, the latter time point was considered as the reference unfed control. Since dogfish appear to feed opportunistically and infrequently in the wild, the 5 days control group roughly approximates baseline physiological conditions (Wood et al., 2007a).

2.2. Tissue sampling and protein extraction

At each sample time (6 h, 20 h, and 5 days post-feeding), fish were terminally anaesthetized in their isolation boxes by an overdose of MS-222 (0.2 g L^{-1}). Rectal glands were dissected immediately and snap frozen in liquid nitrogen. Tissues were then stored at −80 °C, shipped from Bamfield Marine Science Centre, BC (Canada) to Davis, CA (USA) on dry ice, and stored again at −80 °C until protein extraction. Proteins were extracted by first homogenizing tissues in 4 volumes of ND-RIPA buffer composed of 50 mM Tris–HCl (pH 7.6), 150 mM NaCl, 1% (v/v) Triton-X100, 1% (v/v) Nonidet P-40, 1× Complete-Mini™ Protease inhibitor cocktail (Roche), 1 mM NaF, and 1 mM activated Na_3VO_4. Homogenization in tight-fitting glass homogenizers (Wheaton) was performed on ice. Homogenates were centrifuged for 15 min at 19,000 g and 4 °C to pellet debris and other insoluble material. Supernatants were aliquoted into 2 mL siliconized microcentrifuge tubes, and protein concentration was determined using a BCA protein assay (Pierce). The volume of protein extract needed for 1 mg of protein was then precipitated to remove salt and other contaminants in 3 volumes of precooled acetone for 30 min at −20 °C. Precipitated proteins were centrifuged for 5 min at 19,000 g and 4 °C, and then protein pellets were air-dried for 5 min. Proteins were resuspended in 380 μL of IPG rehydration buffer composed of 7 M urea, 2 M thiourea, 2% CHAPS, 0.002% bromophenol blue, 2% Nonidet P-40, 0.5% IPG buffer 3-10NL (ampholyte solution, Amersham), and 100 mM dithioerythritol. Once resuspended in IPG rehydration buffer, samples were immediately used for rehydration of IPG strips.

2.3. Two-dimensional gel electrophoresis (2DGE)

Samples (1.0 mg protein) were added to IPG strips (18 cm, pH range 3–10NL, Bio-Rad) by overnight passive rehydration loading at 20 °C. IPG strips were then processed by isoelectric focusing in two batches in a Protean IEF Cell (Bio-Rad) at 10,000 V for 47,000 Vh. After isoelectric focusing IPG strips were frozen at −80 °C. Second dimension separation of proteins was preceded by two step protein reduction/alkylation and equilibration of IPG strips as previously described (Valkova and Kültz, 2006). Equilibrated IPG strips were loaded on top of uniform 11% polyacrylamide/Bis SDS gels and overlaid with 0.8% low melting point agarose (FMC) containing 0.002% bromophenol blue (Valkova et al., 2005). Six second-dimension gels (16×16×0.15 cm) were then electrophoresed simultaneously by SDS-PAGE at 30 mA per gel constant current and 10 °C using three Protean Xii units (Bio-Rad). Treatment groups were mixed in each second dimension run to minimize systematic variability due to run-specific conditions. After the bromophenol blue dye front had reached the bottom of the gel, staining was performed immediately with colloidal Coomassie blue. Gels were imaged as 16-bit TIFF files with an Epson 1680 densitometer as previously described (Valkova and Kültz, 2006).

2.4. Analysis of protein patterns

Protein spots on all 2D gels were detected and matched using the Group Warp Strategy of Delta 2D gel analysis software (version 3.4, Decodon, Germany). Within each treatment, all gels were warped to a reference gel (containing the most spots). Subsequently, the reference gels for the 6-hour and 20-hour treatments were warped to the reference gel for the 5-days control. A master gel was then created with Delta 2D by fusing all gel images using maximum intensity fusion type, which creates an image that contains all spots present on any gel and each spot at its maximal intensity. Spot detection was then performed on the master gel, and spot boundaries were exported from the master gel to all individual gels to eliminate variability in spot quantification due to spot shape and to ensure 100% spot matching. Ten normalization spots that were equally abundant (expression ratio ~0.9–1.1 when comparing all treatments; Table 1) in all gels/treatments and that were distributed across the master gel were used as a baseline for spot quantification (Lee et al., 2006). Using Delta 2D software, every spot on each gel was quantified, averages for each treatment were calculated, expression ratios were calculated for the 6-hour and 20-hour treatments relative to the 5-days control group, and *t*-test statistics were calculated for each expression ratio. Molecular mass of spots was determined from a nonlinear model fit to the second-dimension migration distances of known molecular mass standards (Precision Plus Protein Standards, Bio-Rad). Isoelectric point (pI) was estimated based on distance from the IPG strip anode.

2.5. In-gel digestion and mass spectrometry (MS)

We limited mass spectrometry analysis to proteins that significantly (*t*-test, $p<0.05$) changed more than 2-fold (i.e., increased more than 100% or decreased more than 50%) in expression/abundance between the reference control and the 6 h and 20 h post-feeding samples. The 2-fold cutoff was chosen for biological relevance and to focus on proteins with maximal variation in expression relative to starved sharks. All spots meeting the expression ratio and statistical criteria, as well as the ten

Table 1
Expression ratios for all dogfish shark rectal gland proteins analyzed by mass spectrometry, including normalization spots (Q1–Q10)

Spot	Protein name	6 h/5 days		20 h/5 days	
		Expression ratio	*p*-value	Expression ratio	*p*-value
Q1	Heat shock protein 60 kDa	0.92	0.530	0.93	0.589
Q2		0.98	0.941	1.02	0.900
Q3	ATP synthase beta chain	0.95	0.712	0.96	0.598
Q4	Alpha enolase	1.00	0.987	0.93	0.718
Q5	Creatine kinase	0.99	0.960	0.93	0.710
Q6	ATP synthase, alpha chain	1.15	0.586	1.07	0.770
Q7	Superoxide dismutase	0.94	0.727	1.13	0.290
Q8	Dihydrolipoyl dehydrogenase, mitochondrial precursor	0.99	0.945	0.98	0.889
Q9	ATP synthase, delta chain	0.87	0.429	0.98	0.864
Q10	ATP synthase, alpha chain	1.13	0.526	1.01	0.961
01/13	Transgelin	**2.48**	**0.008**	**2.14**	**0.009**
02		**3.06**	**<0.001**	**2.63**	**0.002**
03	Voltage-dependent anion channel	1.65	**0.003**	**2.51**	**0.002**
04	Tropomyosin alpha chain	1.17	0.587	**3.08**	**0.011**
05	Tropomyosin alpha chain	1.32	0.301	**2.94**	**0.001**
06		1.79	**0.040**	**2.14**	**0.001**
07/21		**2.42**	**0.013**	**2.30**	**0.026**
08	NADH ubiquinone oxidoreductase 23 kDa subunit	1.18	0.598	**2.22**	**0.024**
09/22	ATP synthase alpha chain, mitochondrial precursor	**3.46**	**0.012**	**2.81**	**0.001**
10		2.10	0.095	**2.22**	**0.001**
11		0.93	0.850	**0.23**	**0.028**
12		0.23	0.056	**0.20**	**0.047**
14		**0.49**	**0.036**	0.63	0.084
15		**0.42**	**0.043**	0.65	0.214
16		**0.49**	**0.035**	0.63	0.105
17	Malate dehydrogenase, mitochondrial	**0.48**	**0.024**	0.53	**0.027**
18	Voltage-dependent anion-selective channel protein 2	**2.06**	**0.017**	1.76	**0.015**
19	NADP-dependent isocitrate dehydrogenase, cytosolic	**2.46**	**0.015**	1.54	0.259
20	Voltage-dependent anion-selective channel protein 2	**2.28**	**0.007**	1.60	**0.044**
23	ATP synthase alpha subunit, isoform 1	**0.37**	**0.046**	0.50	0.106
24		**2.64**	**0.029**	1.39	**0.050**
25		**2.23**	**0.014**	1.75	**0.003**
26	Nucleoside diphosphate kinase	**2.33**	**0.011**	1.47	0.140
27	Malate dehydrogenase, cytosolic	**2.14**	**0.003**	1.51	**0.001**

Ratios were calculated for the 6-hour and 20-hour treatment groups relative to the 5-days control group. Probabilities are given for *t*-tests ($N=5$ per treatment). Bold font indicates proteins that met the statistical ($p<0.05$) criterion, the expression ratio (<0.5 or >2.0) criterion, or both criteria for mass spectrometry analysis for that time point.

normalization spots, were excised from 2D gels using a 1 mm spot puncher. Each of these protein spots was picked in duplicate or triplicate (i.e., the same spot was picked from 2 to 3 2D gels representing rectal gland tissue of 2 to 3 dogfish sharks) for mass spectrometry. Tryptic in-gel digestion and peptide extraction were performed in a dust-free environment at room temperature in 96-well ZipPlates™ (Millipore, Billerica, MA) containing immobilized C18 resin. Peptides were extracted using the centrifugation protocol and the buffers provided in the Montage In-Gel DigestZP Kit (Millipore), with the following modifications: picked spots were incubated for 16 h at 37 °C in 20 μL of diluted ProMega mass spectrometry grade trypsin (2 μg trypsin dissolved in 500 mL of 50 mM NH_4HCO_3) for tryptic digestion; the final peptide elution volume was 4 μL. Eluted protein samples were spotted in one or two 0.5 μL increments on a stainless steel target and they were overlaid with equal amounts of matrix. The matrix, α-cyano-4-hydroxycinnamic acid (HCCA, Sigma, St. Louis, MO), was dissolved at 5 mg/mL in 50:50 acetonitrile:H_2O, which contained 10 mM ammonium phosphate to reduce the intensity of matrix peaks in MS spectra (Zhu and Papayannopoulos, 2003). The HCCA matrix was recrystallized from 70% acetonitrile:30% H_2O prior to use.

Spotted, trypsin-digested proteins were analyzed using matrix-assisted laser desorption/ionization time-of-flight (MALDI-TOF) mass spectrometry on a 4700 Proteomics Analyzer from Applied Biosystems (Foster City, CA) using both MS and tandem MS/MS operating modes. Peptide fragmentation of the 7 or 10 most intense peaks in each MS spectrum was achieved in MS/MS mode by both post-source decay (PSD) and collision-induced dissociation (CID) using atmosphere as the collision gas (Lee et al., 2006). Protein identification from MS and MS/MS m/z peaks was carried out with GPS Explorer software (Applied Biosystems) using the Mascot search algorithm (Perkins et al., 1999) to compare observed peaks with *in silico* digests of proteins in the SwissProt and National Center for Biotechnology Information (NCBI) non-redundant databases. In addition, MS/MS spectra were *de novo* sequenced using the DeNovo Explorer module of GPS Explorer (Applied Biosystems); *de novo* sequences were used to search the NCBI non-redundant database using the MS-BLASTP2 search algorithm (Shevchenko et al., 2001; EMBL). Previous work on this species demonstrated that this *de novo* sequencing approach can be used to identify proteins not matched by peptide mass fingerprint search algorithms such as Mascot (Lee et al., 2006). Mass accuracy limit was set at 50 ppm for MS spectra in each case, and a mass error tolerance of 0.2 Da was used for MS/MS search algorithms. Six criteria were used for successful identification of proteins: (1) Mascot score for peptide mass fingerprinting taking into account matching m/z peaks of MS/MS spectra generated by PSD, (2) Mascot score for peptide mass fingerprinting taking into account matching m/z peaks of MS/MS spectra generated by CID, (3) MS-BLASTP2 score based on *de novo* sequencing of multiple MS/MS peptides generated by PSD, (4) MS-BLASTP2 score based on *de novo* sequencing of multiple MS/MS peptides generated by CID, (5) matching pI on 2D gels, and (6) matching molecular mass on 2D gels (Table 2).

2.6. Bioinformatics analysis of protein functions and pathways

The NCBI sequences of all identified proteins were scored against the PANTHER (Protein ANalysis THrough Evolutionary Relationships v6.0, www.pantherdb.org, Thomas et al., 2003) database of hidden Markov models (HMMs) to determine the homologous PANTHER record for each protein (Mi et al., 2005). A protein list containing the regulated shark proteins was prepared, and the biological processes, molecular functions, and cellular pathways associated with each protein were identified using PANTHER.

2.7. Western blotting and immunodetection

In order to corroborate the protein abundance results of the two-dimensional gel analysis, we selected the NADP-dependent isocitrate dehydrogenase and voltage-dependent anion channel (VDAC) proteins for further analysis by Western blotting. A mouse anti-human polyclonal antibody to cytosolic NADP-dependent IDH was generously provided by Dr. Lee McAlister-Henn and Dr. Karyl Minard (University of Texas Health Science Center at San Antonio, Minard et al., 1998), and a mouse anti-human monoclonal antibody to VDAC protein 2 was obtained from CalBiochem (anti-porin 31HL (AB-2), clone 89-173/025). The VDAC antibody was previously shown to bind specifically to 3–5 isoforms in another elasmobranch species (Shafir et al., 1998). We loaded 40 μg of extracted protein mixture (in RIPA buffer from 2.2. above) into each lane and separated proteins by SDS-PAGE on 11% acrylamide gels. After separation, proteins were blotted onto PVDF membrane. Membranes were blocked in 3% blocking buffer (non-fat milk) and incubated for 2 h in either IDH (1:10,000 dilution) or VDAC antibody (1:5000 dilution). After washing, blots were incubated for 1 h in 3% blocking buffer containing secondary antibody coupled to horseradish peroxidase (1:1000 dilution), developed with SuperSignal Femto (Pierce), and imaged with a ChemiImager (Alpha Innotech, San Leandro, CA). Immunoreactivity was quantified by densitometry using IMAGEQUANT software (Bio-Rad).

3. Results

3.1. Expression ratios following feeding

Using Delta 2D we quantified expression of 684 protein spots that were consistently identifiable and were discernible for spot picking for MS. The two-dimensional gel analysis revealed a number of protein spots that were up or down-regulated following a meal relative to the control (5 days post-feeding) (Table 1, Fig. 1). At 6 h post-feeding, expression of eleven spots was up-regulated 2-fold or more relative to controls, while five proteins decreased significantly in abundance (Fig. 1a). By 20 h post-feeding, 10 spots increased in abundance, and two other proteins had decreased to roughly 20% of their abundance relative to reference controls (Fig. 1b). Four proteins were up-regulated more than 2-fold at both the 6 h and 20 h time points: transgelin, the mitochondrial precursor of ATP synthase alpha chain, and two unidentified proteins.

Table 2
Mass spectrometry (MS) identification scores for dogfish shark rectal gland proteins from Mascot and MS-BLASTP2 database searches

Spot	Protein name	Mascot SwissProt			Mascot NCBInr			MS-BLASTP2 NCBInr			pI (pH units)		M.M. (kDa)		Acc. No.	PANTHER ID
		PSD	CID	Seq. Cov.	PSD	CID	Seq. Cov.	PSD	CID	MS/MS	Theor.	Gel	Theor.	Gel		
Q1	Heat shock protein 60 kDa	159	151	13/17	200	247	21/22	225	147	4/3	5.6	5.2	61.4	55.0	31044489	
Q2												5.0		45.4		
Q3	ATP synthase, beta chain	90	122	29/29	90	122	29/29				6.2	5.1	47.3	44.9	73961223	
Q4	Alpha enolase	125	115	21/18	152	134	17/17	348	402	6/8	5.3	6.1	40.7	40.8	4416383	
Q5	Creatine kinase				180	174	15/18	237	173	4/3	7.8	6.1	34.1	26.6	28630226	
Q6	ATP synthase, alpha chain	137	137	13/13	161	159	15/15	159	161	3/3	9.3	6.4	43.0	21.9	44964389	
Q7	Superoxide dismutase	135	141	6/13	135	141	7/13	269	315	4/5	6.8	6.3	21.4	21.6	41152470	
Q8	Dihydrolipoyl dehydrogenase, mitochondrial precursor	150	158	12/12	235	223	17/17	155	169	3/3	8.2	5.8	54.6	26.1	71897021	
Q9	ATP synthase, delta chain							149		3/	5.1	3.8	16.9	21.2	Q6P1J5	
Q10	ATP synthase, alpha chain	167	135	26/15	174	187	31/9	189	143	3/2	9.1	4.8	60.0	16.1	60552664	
01/13	Transgelin							163	170	3/3	8.9	9.0	22.6	20.2	Q6FI52	PTHR18959: SF5
02												7.6		16.2		
03	Voltage-dependent anion channel				526	560	25/22	514	371	8/6	8.4	9.2	30.6	15.7	7637908	PTHR11743: SF11
04	Tropomyosin alpha chain	177	91	29/27	194	119	41/41	100		2/	4.8	4.3	29.1	33.8	89271378	PTHR19269: SF16
05	Tropomyosin alpha chain	139	150	30/48	177	168	43/49				4.8	4.4	29.1	27.6	64546	PTHR19269: SF16
06												7.9		25.9		
07/21												7.8		26.5		
08	NADH ubiquinone oxidoreductase, 23 kDa subunit	117	128	24/18	125	129	29/41	153	74	3/1	6.5	4.9	24.2	22.4	52782251	PTHR10849
09/22	ATP synthase alpha chain, mitochondrial precursor	99		19/	110		14/				9.3	6.9	43	21.9	44964389	PTHR15184: SF3
10												8.7		21.0		
11												3.4		17.6		
12												5.1		17.7		
14												5.1		53.8		
15												4.8		31.5		
16												5.1		31.3		
17	Malate dehydrogenase, mitochondrial	159	184	13/15	161	188	16/18	262	383	5/7	8.4	7.2	29.9	29.6	89574151	PTHR11540: SF1
18	Voltage-dependent anion-selective channel protein 2	352	357	12/12	352	357	12/12	464	545	7/9	8.6	7.5	30.3	26.5	46048903	PTHR11743: SF12
19	NADP-dependent isocitrate dehydrogenase, cytosolic	79		9/				68	119	1/2	8.4	7.0	50.4	26.6	Q802Y2	PTHR11822
20	Voltage-dependent anion-selective channel protein 2	124	120	14/14	164	140	12/11	249	145	4/2	8.7	6.5	30.2	26.4	62859123	PTHR11743: SF12
23	ATP synthase alpha subunit, isoform 1				97	88	12/9				9.5	6.0	39.6	20.3	28630332	PTHR15184: SF3
24												5.8		19.8		
25												5.4		18.3		
26	Nucleoside diphosphate kinase	114	113	29/35	114	113	29/35	109	88	2/1	8.6	7.5	17.4	18.2	127987	PTHR11349
27	Malate dehydrogenase, cytosolic	82	87	11/9	104	112	12/12	183	180	4/4	6.5	6.5	36.7	21.7	38014771	PTHR23382

MS data using both post-source decay (PSD) and collision-induced dissociation (CID) MS/MS modes were searched against both the SwissProt and NCBInr protein databases. Sequence coverage for peptide mass fingerprinting (in % of overall sequence) are shown for PSD and CID searches. The number of correctly sequenced MS/MS peptides for MS-BLASTP2 searches is also shown (MS/MS). Isoelectric point (p*I*) and molecular mass (M.M.) are presented for both the top database hit (Theoretical) and from 2D gels (Gel). Accession numbers starting with a Q are for SwissProt; all others are for NCBI. Spots Q1–Q10 were normalization proteins for which expression did not change among treatments. The remaining proteins were up- or down-regulated following feeding (Table 1).

3.2. Mass spectrometry identification of proteins

Of the 34 shark proteins analyzed by mass spectrometry, we were able to identify 22 (=65%) with high confidence: 15 using both Mascot and MS-BLASTP2 scores, 4 using Mascot scores only, and 3 using MS-BLASTP2 scores only (Table 2). All identified proteins were positively identified from at least two separate 2D gels (i.e., from more than one shark). Nine of the ten

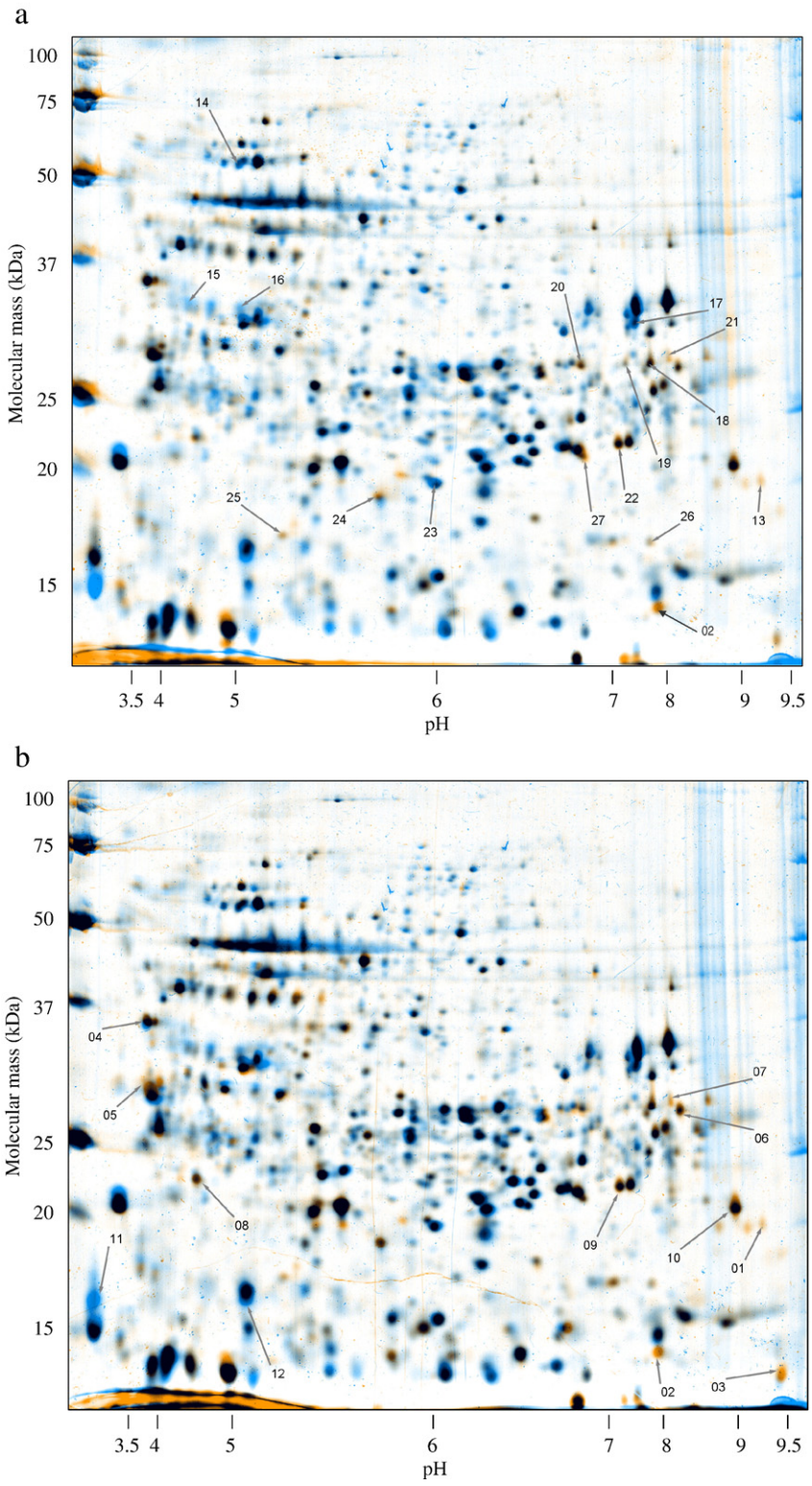

Fig. 1. Two-dimensional gel image overlays depicting relative protein expression following a meal in dogfish shark rectal gland. (a) 5 days (control, blue) vs. 6 h following a meal (orange). (b) 5 days (control, blue) vs. 20 h following a meal (orange). Images are composite averages of 5 individual shark gels at each timepoint, created with Delta 2D software. Black spots are equally expressed at both time points; colored spots indicate higher mean expression at the corresponding time point. Protein spots with statistically significantly different expression levels between the two time points are indicated by numbered arrows (see Tables 1 and 2).

normalization spots were identified; these included HSP 60, alpha enolase, creatine kinase, and superoxide dismutase. The database searches identified 13 of the proteins that changed following feeding (Table 2). Identified proteins, identification scores, pI and MW, and accession numbers of the closest orthologs are summarized for all identified protein spots in Table 2. Not all

identified proteins matched all six measures; pI and MW, in particular, varied between dogfish shark proteins and the closest orthologs. In addition, high quality mass spectra and *de novo* sequence information were obtained for many of the other analyzed protein spots, but these data did not match entries in the databases searched. This discrepancy between observed shark protein characteristics and database entries is likely the result of variation in amino acid sequence between shark proteins and orthologous proteins in species with sequenced genomes.

Interestingly, there were several instances where two or more isoforms or posttranslational modification (PTM) variants of a given protein were regulated following feeding (i.e., more than one spot gave the same protein ID). Two isoforms/PTM variants of tropomyosin alpha chain were up-regulated at 20 h following feeding; 3 isoforms/PTM variants of voltage-dependent anion-selective channel were up-regulated to varying degrees at both 6 h and 20 h (including a sequenced dogfish isoform; Fig. 2); and ATP synthase alpha subunit decreased in abundance following feeding, while the mitochondrial precursor of ATP synthase alpha chain increased in abundance. In addition, the mitochondrial form of malate dehydrogenase decreased in abundance following feeding, while the cytosolic form increased in abundance (Table 1).

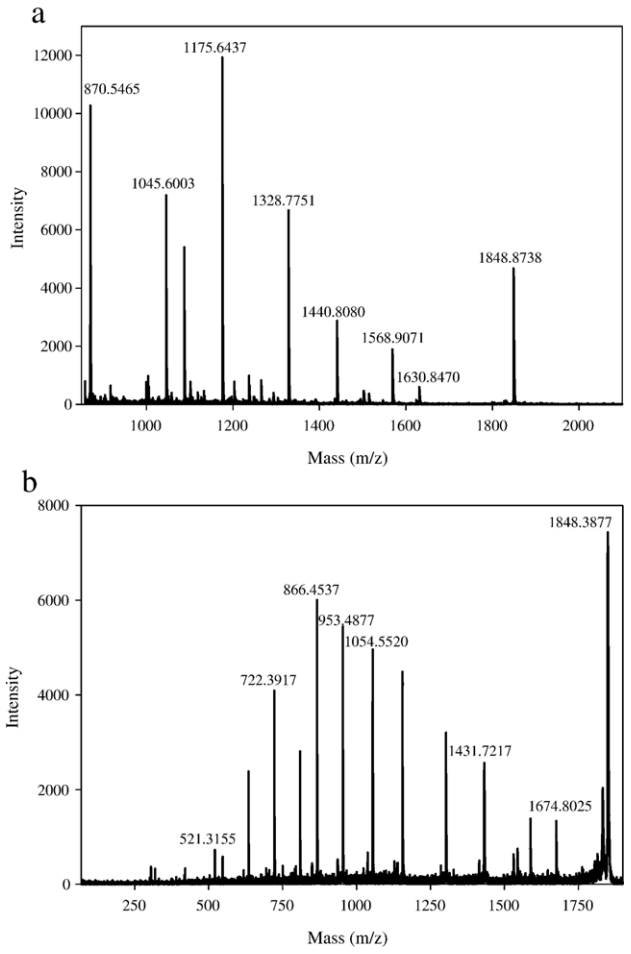

Fig. 2. Mass spectrometry data for protein spot 03 that was identified as voltage-dependent anion channel of *Squalus acanthias* with a Mascot score of 560 (see Table 2). This protein has been sequenced for *Squalus acanthias* (Schröder et al., 2000), and its sequence is present in the NCBInr database. (a) MS spectrum showing peptide ion masses resulting from tryptic digestion of spot 03. (b) MS/MS spectrum of the parent ion at m/z 1848 obtained in collision-induced dissociation (CID) mode. This MS/MS spectrum was annotated by DeNovo Explorer, yielding the amino acid sequence SSSGVEMTTSGSSNTDTGK for this peptide.

3.3. Functional classification of proteins regulated after feeding

All but one (voltage-dependent anion channel isoform from dogfish shark; NCBI accession number 7637908) of the 13 identified proteins regulated by feeding had corresponding PANTHER entries (Table 2). These 12 proteins were classified into 8 molecular functions: ion channel, kinase, oxidoreductase, receptor, synthase, transporter, cytoskeletal protein, and hydrolase. The proteins were also assigned to 7 biological processes: cell structure and motility, carbohydrate metabolism, transport, muscle contraction, nucleoside metabolism, electron transport, and developmental processes. Five protein spots yielded hits with three PANTHER pathways: ATP synthase alpha chain and its mitochondrial precursor (ATP synthesis pathway), nucleoside diphosphate kinase (*de novo* purine biosynthesis pathway), the cytosolic form of malate dehydrogenase (TCA cycle), and NADP-linked isocitrate dehydrogenase (TCA cycle). However, the latter classification pertains to the mitochondrial isoform of isocitrate dehydrogenase, while our MS analysis and a subsequent sequence comparison identified the cytosolic isoform of NADP-dependent isocitrate dehydrogenase (Table 2). This cytosolic isoform is more likely involved in supplying reducing equivalents for biosynthesis (e.g., Minard et al., 1998).

3.4. Western blots for cytosolic NADP-dependent IDH and VDAC

The immunoreactivity volume of the single cytosolic NADP-dependent IDH band increased significantly in the 6 h treatment relative to the 5 day controls, while there was no significant change in this protein at 20 h (Fig. 3a and b). These results agree with the two-dimensional gel analysis (Table 1). The VDAC antibody bound strongly to two different isoforms of ~27 and ~26 kDa molecular mass on one-dimensional gels; a third VDAC band at ~15–17 kDa was faintly but unreliably detected (Fig. 3c). Both larger isoforms showed a trend toward increased immunoreactivity volumes at 6 and 20 h relative to 5 days, as was observed in the two-dimensional gel analysis, but these increases were not statistically significant (Fig. 3d).

4. Discussion

The identified proteins that were up- or down-regulated following feeding in the dogfish shark rectal gland fell primarily into three broad categories: cytoskeletal/muscular (e.g., tropomyosin alpha chain, transgelin), energy metabolism (e.g., ATP synthase, malate dehydrogenase), and nucleotide metabolism. With respect to energy metabolism, up-regulated proteins represented either specific enzymes of the tricarboxylic acid cycle/electron transport system, or enzymes that support NADH

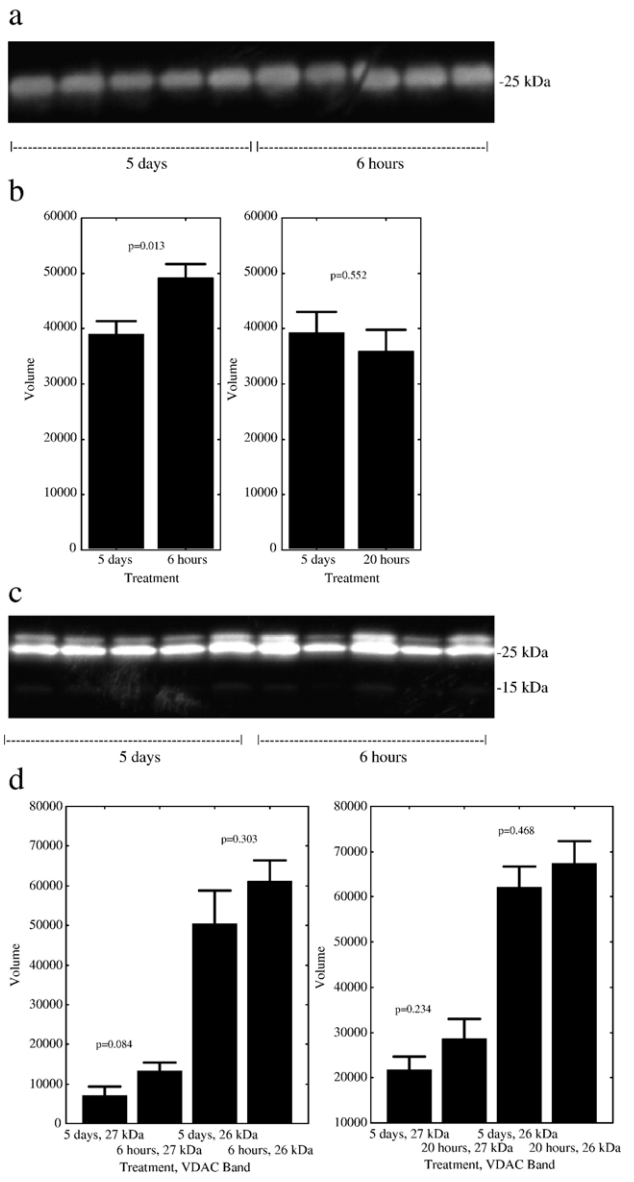

Fig. 3. Representative Western blots and immunoreactivity band volumes for cytosolic NADP-dependent isocitrate dehydrogenase (IDH) and voltage-dependent anion channel (VDAC) in dogfish shark rectal gland after feeding. a) Western blot for IDH depicting single band at ~25 kDa. b) IDH immunoreactivity at 5 days (control), 6 h, and 20 h following a meal. c) Western blot for VDAC demonstrating presence of two strong bands at ~26–27 kDa and a very faint band at ~15–17 kDa. d) Immunoreactivity of the two larger isoforms of VDAC at 5 days (control), 6 h, and 20 h following a meal. Statistical *p*-values are for Student's *T*-test.

oxidation or redox balance by allowing shuttling of reducing equivalents between the cytosol and mitochondria. In addition, Schröder et al. (2000) sequenced the dogfish shark voltage-dependent anion channel gene, and they suggested a conserved role for this outer mitochondrial membrane porin in ATP synthesis and energy production in the rectal gland. Collectively, these results suggest that maintaining the cellular supply of energy is a critical component of the rectal gland's response to activation by feeding. These results are in accord with increased secretory and metabolic activity of the dogfish rectal gland following feeding (MacKenzie et al., 2002; Walsh et al., 2006), which requires significant energy to power the Na^+/K^+-ATPase pumps that drive salt excretion.

In the case of isocitrate dehydrogenase, the current approach was able to demonstrate that the previously observed increase in NADP-specific IDH activity (Walsh et al., 2006) was achieved, at least in part, by an increase in protein quantity. In the prior measurements of activity, however, Walsh et al. (2006) did not determine if the increase was in the mitochondrial IDH, the cytoplasmic IDH, or both. The peptide sequence obtained by MS in the present study *did* enable ready distinction from the mitochondrial NADP-specific IDH, and further analysis of potential codon utilization allowed us to tentatively determine that the cytoplasmic NADP-specific form was up-regulated. Our Western blot analysis using an antibody specific to cytosolic NADP-specific IDH corroborated this result, demonstrating a significant increase in immunoreactivity at 6 h after a meal. However, future studies might isolate mitochondria from rectal glands of fed vs. unfed dogfish, and compare mitochondrial and cytoplasmic fractions for both IDH activity and specific protein quantities, to fully characterize this aspect of the rectal gland's response to feeding.

The increases in the quantities of proteins in the cytoskeletal/muscular category (transgelin and tropomyosin alpha chain) are rather interesting, implicating muscular/morphological activity as an important component of the rectal gland's response to salt load after feeding. It has been suggested previously that rectal gland secretion rate may be controlled by changes in cell volume (e.g., Greger et al., 1999) and/or blood perfusion via the posterior mesenteric artery supplying the gland, and that this vasculature may be tonically constricted when the gland is inactive (see e.g., Shuttleworth, 1988). Furthermore, microscopic studies (reviewed by Olson, 1999) have described an inner muscular layer within the gland itself, between the secretory tubules and connective tissue layer of the outer capsule (e.g., Bulger, 1963). More recently, Evans and Piermarini (2001) were able to confirm the presence of this muscle ring in rectal glands of three elasmobranch species, including *S. acanthias*, and they suggested that morphological/dimensional changes in the gland may play an important role in secretion. Notably, they were able to demonstrate that isolated rectal gland rings constricted *in vitro* in response to applications of acetylcholine, endothelin, and nitric oxide. Our data for increases in abundances of cytoskeletal/muscular proteins would appear to support this notion. The fed/starved dogfish model used in the present study would appear to be ideally suited to further examine the role of rectal gland morphological changes in salt secretion.

The discrepancy between shark and "model organism" proteins, and our failure to identify all proteins analyzed in this study, was to be expected since a single amino acid difference may significantly alter the molecular mass of a tryptic peptide and hinder Mascot identification. Nevertheless, our data illustrate that MS-BLASTP2 matching of multiple *de novo* peptide sequences obtained by MS/MS, in concert with peptide mass fingerprinting searches such as Mascot, represents a powerful and complementary approach for identification of proteins from non-model organisms. Once an elasmobranch genome is sequenced and annotated (the little skate, *Leucoraja*

erinacea, is currently assigned to Washington University in St. Louis sequencing center), it will be possible to identify numerous additional shark proteins based on sequence similarity, including some or all of the dozen protein spots that changed expression here but that were not identified (Table 1).

Overall, our data taken in concert with those of Walsh et al. (2006) indicate that substantial changes in protein expression are effected in the rectal gland by feeding. Interestingly, quite a few proteins exceeded the criterion of a 2-fold change at only 6 h post-feeding. Since these changes would appear to take place at the transcriptional/translational level (or via slower degradation of high-turnover proteins), these results imply either a very rapidly induced, coordinated combination of transcription and translation, or perhaps rapid translation of pre-existing message. Since transcriptomic approaches are now becoming more routine, it would be interesting to compare feeding-induced changes in the proteome with potential changes in the transcriptome by these mRNA-based analyses, with particular attention to the time course of early vs. late changing genes/proteins. Interestingly, we did not find obvious evidence for changes in protein content for the many transporters known to be involved in actual salt secretion (e.g., Na^+/K^+-ATPase, NKCC, the apical Cl^- channel, etc.). However, these proteins tend to be large (>100 kDa) and integrated into membranes, both of which characteristics are typically biased against in two-dimensional gel electrophoresis studies without prefractionation approaches. It is also possible that some transporter proteins are among the unidentified ones, or perhaps they are regulated largely by post-translational modification in this context. Additional studies of these proteins (e.g., using alternative methods to two-dimensional gel electrophoresis) and mRNA will be required to distinguish between the different modes and timing of regulation. It would also be of interest to compare those proteins/transcripts responding to feeding with those responding to the independent stimuli of alkalosis vs. volume/salt loading to attempt to understand which stimuli predominate *in vivo*.

Acknowledgements

This project was supported by grant number IOB-0542755 from the National Science Foundation to DK. WWD was supported by a UC Davis Graduate Scholar Fellowship and Block Grant Fellowship. CMW and PJW were both supported by NSERC Discovery grants and the Canada Research Chair Program. We thank Dr. Tom Mommsen for his assistance with sequence analysis of IDH. Dr. Mommsen, Dr. Joseph J. Cech, Jr., and two anonymous reviewers provided helpful comments on an earlier draft of this manuscript. We also thank Dr. Lee McAlister-Henn and Dr. Karyl Minard for providing the IDH antibody.

References

Bulger, R.E., 1963. Fine structure of the rectal (salt-secreting) gland of the spiny dogfish, Squalus acanthias. Anat. Rec. 147, 95–127.

Evans, D.H., Piermarini, P.M., 2001. Contractile properties of the elasmobranch rectal gland. J. Exp. Biol. 204, 59–67.

Fellner, S.K., Parker, L., 2002. A Ca2+-sensing receptor modulates shark rectal gland function. J. Exp. Biol. 205, 1889–1897.

Fellner, S.K., Parker, L., 2004. Ionic strength and the polyvalent cation receptor of shark rectal gland and artery. J. Exp. Zool. 301A, 235–239.

Greger, R., Heitzmann, D., Hug, M.J., Hoffmann, E.K., Bleich, M., 1999. The Na+, 2Cl−, K+ cotransporter in the rectal gland of Squalus acanthias is activated by cell shrinkage. Eur. J. Physiol. 438, 165–176.

Hazon, N., Wells, A., Pillans, R.D., Good, J.P., Anderson, W.G., Franklin, C.E., 2003. Urea based osmoregulation and endocrine control in elasmobranch fish with special reference to euryhalinity. Comp. Biochem. Physiol. B 136, 685–700.

Lee, J., Valkova, N., White, M.P., Kultz, D., 2006. Proteomic identification of processes and pathways characteristic of osmoregulatory tissues in spiny dogfish shark (Squalus acanthias). Comp. Biochem. Physiol. D 1, 328–343.

MacKenzie, S., Cutler, C.P., Hazon, N., Cramb, G., 2002. The effects of dietary sodium loading on the activity and expression of Na, K-ATPase in the rectal gland of the European Dogfish (Scyliorhinus canicula). Comp. Biochem. Physiol. B 131, 185–200.

Mi, H., Lazareva-Ulitsky, B., Loo, R., Kejariwal, A., Vandergriff, J., Rabkin, S., Guo, N., Muraganujan, A., Doremieux, O., Campbell, M.J., Kitano, H., Thomas, P.D., 2005. The PANTHER database of protein families, subfamilies, functions and pathways. Nucleic Acids Res. 33, D284–D288.

Minard, K.I., Jennings, G.T., Loftus, T.M., Xuan, D., McAlister-Henni, L., 1998. Sources of NADPH and expression of mammalian NADP1-specific isocitrate dehydrogenases in Saccharomyces cerevisiae. J. Biol. Chem. 273, 31486–31493.

Olson, K.R., 1999. Rectal gland and volume homeostasis. In: Hamlett, W.C. (Ed.), Sharks, Skates, and Rays. Johns Hopkins University Press, Baltimore, pp. 329–352.

Perkins, D.N., Pappin, D.J.C., Creasy, D.M., Cottrell, J.S., 1999. Probability-based protein identification by searching sequence databases using mass spectrometry data. Electrophoresis 20, 3551–3567.

Riordan, J.R., Forbushi, B.I., Hanrahan, J.W., 1994. The molecular basis of chloride transport in shark rectal gland. J. Exp. Biol. 196, 405–418.

Schröder, A.K., Aller, S.G., Forrest Jr., J.N., 2000. Cloning of a mitochondrial voltage-dependent anion channel from the shark rectal gland. Bull. Mt. Desert Isl. Biol. Lab. 38, 133–135.

Shafir, I., Feng, W., Shoshan-Barmataz, V., 1998. Voltage-dependent anion channel proteins in synaptosomes of the torpedo electric organ: immuno-localization, purification, and characterization. J. Bioenerg. Biomembranes 30, 499–510.

Shevchenko, A., Sunyaev, S., Loboda, A., Shevchenko, A., Bork, P., Ens, W., Standing, K.G., 2001. Charting the proteomes of organisms with unsequenced genomes by MALDI-quadrupole time-of-flight mass spectrometry and BLAST homology searching. Anal. Chem. 73, 1917–1926.

Shuttleworth, T.J., 1988. Salt and water balance – extrarenal mechanisms. In: Shuttleworth, T.J. (Ed.), Physiology of Elasmobranch Fishes. Springer-Verlag, Berlin, pp. 171–199.

Shuttleworth, T.J., Thompson, J., Munger, R.S., Wood, C.M., 2006. A critical analysis of carbonic anhydrase function, respiratory gas exchange, and the acid-base control of secretion in the rectal gland of Squalus acanthias. J. Exp. Biol. 209, 4701–4716.

Silva, P., Solomon, R.J., Epstein, F.H., 1990. Shark rectal gland. Methods Enzymol. 192, 754–766.

Silva, P., Solomon, R.J., Epstein, F.H., 1996. The rectal gland of Squalus acanthias: a model for the transport of chloride. Kidney Int. 49, 1552–1556.

Solomon, R.J., Taylor, M., Rosa, R., Silva, P., Epstein, F.H., 1984a. In vivo effect of volume expansion on rectal gland function II. Hemodynamic factors. Am. J. Physiol. 246, R67–R71.

Solomon, R.J., Taylor, M., Stoff, J.S., Silva, P., Epstein, F.H., 1984b. In vivo effect of volume expansion on rectal gland function I. Humoral factors. Am. J. Physiol. 246, R63–R66.

Solomon, R.J., Taylor, M., Sheth, S., Silva, P., Epstein, F.H., 1985. Primary role of volume expansion in stimulation of rectal gland function. Am. J. Physiol. 248, R638–R640.

Thomas, P.D., Campbell, M.J., Kejariwal, A., Mi, H., Karlak, B., Daverman, R., Diemer, K., Muruganujan, A., Narechania, A., 2003. PANTHER: a library of protein families and subfamilies indexed by function. Genome Res. 13, 2129–2141.

Valkova, N., Kültz, D., 2006. Constitutive and inducible stress proteins dominate the proteome of the murine inner medullary collecting duct-3 (mIMCD3) cell line. Biochim. Biophys. Acta 1764, 1007–1020.

Valkova, N., Yunis, R., Mak, S., Kang, K., Kültz, D., 2005. Nek8 mutation causes overexpression of galectin-1, sorcin, and vimentin and accumulation of the major urinary protein in renal cysts of jck mice. Mol. Cell. Proteomics 4, 1009–1018.

Walsh, P.J., Kajimura, M., Mommsen, T.P., Wood, C.M., 2006. Metabolic organization and effects of feeding on enzyme activities of the dogfish shark (Squalus acanthias) rectal gland. J. Exp. Biol. 209, 2929–2938.

Wood, C.M., Kajimura, M., Mommsen, T.P., Walsh, P.J., 2005. Alkaline tide and nitrogen conservation after feeding in an elasmobranch (Squalus acanthias). J. Exp. Biol. 208, 2693–2705.

Wood, C.M., Kajimura, M., Bucking, C.P., Walsh, P.J., 2007a. Osmoregulation, ionoregulation and acid-base regulation by the gastrointestinal tract after feeding in the elasmobranch (Squalus acanthias). J. Exp. Biol. 210, 1335–1349.

Wood, C.M., Munger, R.S., Thompson, J., Shuttleworth, T.J., 2007b. Control of rectal gland secretion by blood acid-base status in the intact dogfish shark (Squalus acanthias). Respir. Physiol. Neurobiol. 156, 220–228.

Zhu, X., Papayannopoulos, I.A., 2003. Improvement in the detection of low concentration protein digests on a MALDI TOF/TOF workstation by reducing α-cyano-4-hydroxycinnamic acid adduct ions. J. Biomol. Technol. 14, 298–307.